Short-Term Behavior and Steady-State Value of BHE Thermal Resistance

A. Priarone[1] and S. Lazzari[*2]
[1] DIME-TEC, University of Genova; [2] DIN, University of Bologna
*Corresponding author: Viale Risorgimento 2, I-40136, Bologna, Italy; stefano.lazzari@unibo.it

Abstract: The transient behavior of the thermal resistance of single and double U-tube BHEs is investigated numerically by means of COMSOL Multiphysics with reference to the 2D cross section of usually employed BHEs. The study is performed in a dimensionless parametrical form, the parameters being the ratio between the thermal conductivities of grout and ground, the ratio between the heat capacities per unit volume of grout and ground and the distance between the tubes. The results show that the pipe spacing and the heat capacity ratio play an important role in the transient behavior of the BHE internal resistance, whereas the pipe spacing and the conductivity ratio play an important role in the steady value of the BHE thermal resistance.

Keywords: BHE thermal resistance, short-term analysis, *g*-functions.

1. Introduction

In order to study the thermal behavior of Borehole Heat Exchangers (BHEs), the most employed model is based on two thermal resistances, namely the BHE thermal resistance and the ground thermal resistance [1-4]. Usually, the first one is assumed to be uniform along the whole BHE and constant in time. However, when considering the short-term behavior of the BHE, this assumption is quite rough and can lead to relevant discrepancies with respect to the real BHE performance. Indeed, the heat capacity of the grout cannot be neglected in hourly simulations. In Ref.[5], the Authors proposed a new method for the hourly simulation of BHE fields, where the internal structure of the BHE is also taken into account. The present paper complements Ref.[5] being a transient parametrical study of the grout thermal resistance of the BHE, *i.e.*, the resistance between the tubes and the ground. This resistance is determined in a dimensionless form by considering both single and double U-tube BHE configurations with different values of the shank-spacing between the tubes. The considered geometrical configurations are based on commercially available geothermal probes [6].

2. Governing Equations and Numerical Model

As well known, in the short time period the BHE length does not affect the BHE thermal response and, thus, the *g*-functions can be determined by 2D numerical simulations performed on a cross section of the BHE. On the contrary, in the short time period the real internal structure of the BHE plays an important role and must be properly taken into account.

Let us consider either a double U-tube BHE or a single U-tube BHE, and denote by D the diameter of the BHE, by D_t the external diameter of each tube and by d the distance between the axes of opposite tubes. The dimensionless parameters used to define the cross section of the BHE are $D_t^* = D_t/D$ and $d^* = d/D$. The values considered for the geometrical parameters are chosen with reference to widely employed double and single U-tube BHEs, and are summarized in Table 1. In detail, two double U-tube BHEs are studied, which are characterized by D_t equal to 32 mm (case *I*) and 40 mm (case *II*), respectively. When the corresponding suggested spacer is used [6], the distance d is 83 mm and 90 mm, respectively; accordingly, the needed perforation diameter D results equal to 127 mm (5") and 152 mm (6"), respectively. Moreover, three configurations of single U-tube BHE are considered, which have the same tube diameter, D_t = 40 mm, and differ only for the distance d, namely: d = 90 mm (case *III*); $d = D_t = 40$ mm (case *IV*, *i.e.*, the tubes are in direct contact); $d = D - D_t = 112$ mm (case *V*, *i.e.*, the tubes are adjacent to the BHE external boundary).

Figure 1 presents a sketch of the cross sections considered for double U-tube BHEs (cases *I* and *II*), whereas figure 2 shows the three configurations of the single U-tube BHE (cases *III*, *IV*, *V*).

Table 1. Geometrical properties of the considered BHE configurations.

	double U-tube BHE		**single U-tube BHE**		
case	***I***	***II***	***III***	***IV***	***V***
D_t [mm]	32	40	40	40	40
d [mm]	83	90	90	40	112
D [mm]	127 (5”)	152 (6”)	152 (6”)	152 (6”)	152 (6”)
$d^* = d/D$	0.6535	0.5921	0.5921	0.2632	0.7368
$D_t^* = D_t/D$	0.2520	0.2632	0.2632	0.2632	0.2632

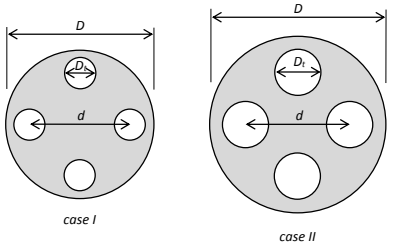

Figure 1. Sketches of the considered cross sections of double U-tube BHEs.

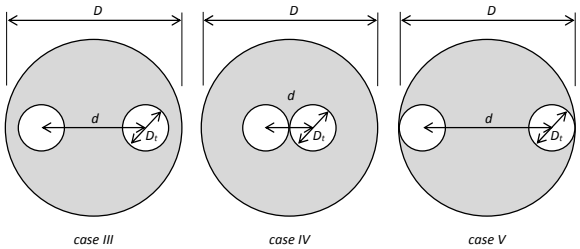

Figure 2. Sketches of the considered cross sections of single U-tube BHEs.

The differential equations to be solved in grout and ground are, respectively:

$$\frac{\partial T}{\partial \tau} = \frac{k_{gt}}{(\rho c)_{gt}} \nabla^2 T \qquad (1)$$

$$\frac{\partial T}{\partial \tau} = \frac{k_{g}}{(\rho c)_{g}} \nabla^2 T \qquad (2)$$

where T is temperature, τ is time, k_{gt} and $(\rho c)_{gt}$ are the thermal conductivity and the heat capacity per unit volume of the grout, while k_g and $(\rho c)_g$ are the thermal conductivity and the heat capacity per unit volume of the ground.

The boundary condition at the surface between tubes and grout is

$$-k_{gt}\left(\nabla T \cdot \mathbf{n}\right)\Big|_S = \frac{Q_0}{4\pi D_t} \qquad (3)$$

where Q_0 is a constant reference heat load per unit length, which begins at the initial instant $\tau = 0$; S is the surface between tubes and grout and **n** denotes the outward unit normal.

The external boundary of the computational domain, which is a circle with radius r_d, is considered isothermal

$$T = T_g \qquad (4)$$

where T_g is the undisturbed ground temperature. Continuity conditions hold at the interface grout-ground, and the initial condition is $T = T_g$ on the whole computational domain.

Let us define the dimensionless temperature T^* and the dimensionless time $\tau^* = Fo_D$ as follows:

$$T^* = k_g \frac{T - T_g}{Q_0}, \quad \tau^* = \frac{k_g \tau}{(\rho c)_g D^2} = Fo_D \qquad (5)$$

By introducing also the dimensionless operator $\nabla^* = D\,\nabla$ and the dimensionless quantities

$$k^* = \frac{k_{gt}}{k_g}, \ (\rho c)^* = \frac{(\rho c)_{gt}}{(\rho c)_g} \qquad (6)$$

one can rewrite Eqs. (1), (2), (3) and (4) in the following dimensionless form:

$$\frac{\partial T^*}{\partial \tau^*} = \frac{k^*}{(\rho c)^*} \nabla^{*2} T^* \qquad (7)$$

$$\frac{\partial T^*}{\partial \tau^*} = \nabla^{*2} T^* \qquad (8)$$

$$-\left(\nabla^* T^* \cdot \mathbf{n}\right)\Big|_{S^*} = \frac{1}{4\pi k^* D_t^*} \quad , \qquad (9)$$

$$T^* = 0 \qquad (10)$$

where S^* denotes the surface between tubes and grout in the dimensionless domain. The dimensionless initial condition is $T^* = 0$ everywhere in the domain.

The dimensionless Eqs. (7)-(10), with the continuity conditions at the interface grout-ground and the initial condition, are solved by means of COMSOL Multiphysics 4.3b.

For all the geometrical configurations considered (cases *I-V*), a circular computational domain with dimensionless radius $r_d/D = 1000$ is

employed; an extensive check of the adequacy of this size of the computational domain has been already performed in Ref. [5], which we refer.

A dimensionless time interval $10^{-4} \leq \tau^* \leq 10^5$ is considered, in the logarithmic scale $-4 \leq \log_{10} \tau^* \leq 5$, which is divided into 4500 uniform time steps (each dimensionless time interval is equal to 0.002).

The dimensionless average temperature at the interface tubes-grout and that at the interface grout-ground, called *g*-functions at those surfaces are evaluated and denoted, respectively, by g_{gt} and g_b. Moreover, we denote the difference $g_{gt} - g_b$ as g_{Rgt}: according to Eq.(5) and to the usual definition of thermal resistance, *i.e.*, $R = \Delta T/Q$, this difference is representative of the dimensionless grout thermal resistance per unit length.

In order to account for the typical ranges of the physical properties of grout and ground, calculations have been performed by considering all the combinations of the following values: $k^* = 0.4, 0.7, 1.0$; $(\rho c)^* = 0.4, 0.7, 1.0$.

To check the mesh independence of results, the function g_{Rgt} has been evaluated by means of four unstructured triangular meshes, obtained with an element size "extremely fine" inside the BHE and "finer" in the ground, which differ for the number of uniformly spaced elements on each tube's boundary and BHE's boundary and, thus, for the overall elements number. For instance, with reference to case *I*, $k^* = 0.4$ and $(\rho c)^* = 0.4$, the four considered meshes are characterized by the following increasing numbers of elements, respectively: 7, 25 and 7624 elements (mesh1); 10, 30 and 8310 elements (mesh2); 15, 50 and 12266 elements (mesh3); 20, 70 and 16858 elements (mesh4). By comparing two successive meshes by means of the following relative absolute error,

$$\varepsilon_{i+1,\,i} = \left| \frac{g_{Rgt\ \,i+1} - g_{Rgt\ \,i}}{g_{Rgt\ \,i+1}} \right| \% \quad i=1,2,3 \qquad (11)$$

we obtained the following percent values: $\varepsilon_{2,1} = 0.215\%$; $\varepsilon_{3,2} = 0.338\%$; $\varepsilon_{4,3} = 0.197\%$. Therefore, as a compromise between accuracy and computational time, mesh3 was adopted for final computations.

3. Discussion of the Results

For every combination of values of the dimensionless parameters $k^* = 0.4, 0.7, 1.0$ and $(\rho c)^* = 0.4, 0.7, 1.0$ and for each BHE considered, the dimensionless average temperature at the interface tubes-grout, namely the *g*-function g_{gt}, and the dimensionless average temperature at the interface grout-ground, namely the *g*-function g_b, have been determined as functions of the dimensionless time Fo_D.

Figure 3 shows the plots of g_{gt} for a double U-tube BHE with $D_t^* = 0.2520$ (case *I*): for a given value of k^*, in the short-term period (*i.e.*, for low values of Fo_D), as the value of $(\rho c)^*$ increases the value of g_{gt} decreases. On the other hand, as Fo_D increases, the curves approach and tend to a common value, which is a decreasing function of k^*.

Figure 4 shows the plots of $g_{Rgt} = g_{gt} - g_b$ for the same BHE (case *I*): for given values of k^*, there exists a threshold value of Fo_D such that the curves become independent of both $(\rho c)^*$ and Fo_D, *i.e.*, the steady-state regime is reached. Indeed, this constant value of g_{Rgt} represents the dimensionless steady-state grout thermal resistance per unit length, which is a decreasing function of k^*.

Analogous considerations can be drawn for the other investigated BHEs (cases *II*-*V*), since the trends of g_{gt} and g_{Rgt} are similar to those shown in Figures 3 and 4.

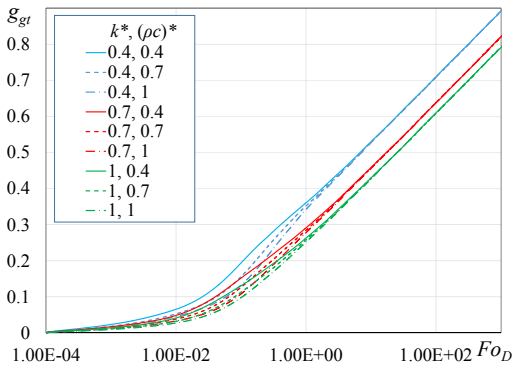

Figure 3. Plots of the *g*-function g_{gt} as a function of Fo_D (case *I*).

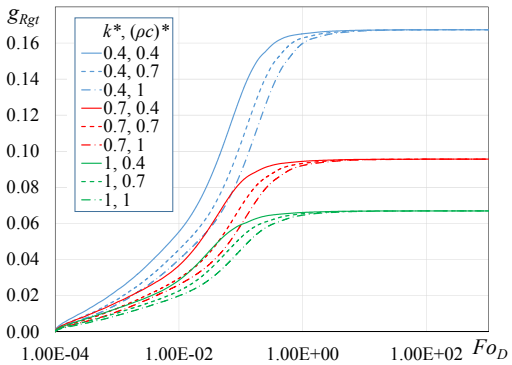

Figure 4. Plots of the *g*-function g_{Rgt} as a function of Fo_D (case *I*).

For each BHE and for given values of k^* and $(\rho c)^*$, the threshold value of Fo_D has been determined as the first value of Fo_D from which the absolute relative difference ε_{FoD} between the values of g_{Rgt} evaluated in two successive dimensionless time instants (the considered time step is 0.002) becomes smaller than 0.001%, namely when:

$$\varepsilon_{FoD} = \left| \frac{g_{Rgt}\left(Fo_D + 0.002\right) - g_{Rgt}\left(Fo_D\right)}{g_{Rgt}\left(Fo_D\right)} \right| \% \quad (12)$$
$$< 0.001\%$$

Table 2 reports the threshold values of Fo_D and the corresponding values of the dimensionless steady-state grout thermal resistance per unit length (in italic), for all the geometrical configurations considered and for all the combinations of the parameters k^* and $(\rho c)^*$.

It is interesting now to compare the thermal response factors, *i.e.*, the *g*-functions, of the two double U-tube BHEs examined in order to compare the corresponding thermal resistances per unit length.

With reference to cases *I* and *II*, for $k^* = 0.7$, Figures 5 and 6 present the plots of g_{gt} and the plots of g_{Rgt}, respectively. Except for the very first dimensionless instants, *i.e.*, for (about) $Fo_D < 8 \cdot 10^{-3}$, Figure 5 shows that the values of g_{gt} and of g_{Rgt} for the BHE with the 40 mm tubes (case *II*) are bigger than those for the BHE with the 32 mm tubes (case *I*).

Table 2. Threshold values of Fo_D and steady-state value of g_{Rgt} (in italic).

Case *I*: double U-tube BHE 32 mm			
	$(\rho c)^* = 0.4$	$(\rho c)^* = 0.7$	$(\rho c)^* = 1$
$k^* = 0.4$	7.62	11.3	16.3
	0.167		
$k^* = 0.7$	6.49	12.0	17.5
	0.095		
$k^* = 1$	6.58	12.2	17.9
	0.067		
Case *II*: double U-tube BHE 40 mm			
	$(\rho c)^* = 0.4$	$(\rho c)^* = 0.7$	$(\rho c)^* = 1$
$k^* = 0.4$	5.20	10.3	16.7
	0.211		
$k^* = 0.7$	5.08	9.73	19.9
	0.120		
$k^* = 1$	5.22	9.86	14.1
	0.084		
Case *III*: single U-tube BHE 40 mm (suggested shank-spacing)			
	$(\rho c)^* = 0.4$	$(\rho c)^* = 0.7$	$(\rho c)^* = 1$
$k^* = 0.4$	3.89	8.02	14.7
	0.235		
$k^* = 0.7$	5.08	7.59	11.2
	0.137		
$k^* = 1$	5.01	7.08	10.3
	0.097		
Case *IV*: single U-tube BHE 40 mm (tubes in direct contact)			
	$(\rho c)^* = 0.4$	$(\rho c)^* = 0.7$	$(\rho c)^* = 1$
$k^* = 0.4$	2.37	3.91	6.85
	0.524		
$k^* = 0.7$	2.82	4.39	7.31
	0.299		
$k^* = 1$	3.12	4.79	6.98
	0.210		
Case *V*: single U-tube BHE 40 mm (tubes adjacent to the BHE external boundary)			
	$(\rho c)^* = 0.4$	$(\rho c)^* = 0.7$	$(\rho c)^* = 1$
$k^* = 0.4$	4.09	7.73	13.9
	0.176		
$k^* = 0.7$	3.53	7.11	12.4
	0.107		
$k^* = 1$	3.10	5.45	9.82
	0.078		

In particular, from Figure 6 one can infer that the ratio between the constant values reached by g_{Rgt} in the two cases is

$$\left(g_{Rgt\ II} / g_{Rgt\ I} \right)_{steady-state} = 1.266 \quad (13)$$

According to the meaning of g_{Rgt}, *i.e.*, $g_{Rgt} = k_g \cdot R'_{gt}$, this is also the value of the ratio between the corresponding grout thermal resistances per unit length:

$$\left(R'_{gt\ II} / R'_{gt\ I}\right)_{steady-state} = 1.266 \qquad (14)$$

The ratio is a slightly increasing function of k^*, being 1.264 for $k^* = 0.4$ and 1.269 for $k^* = 1$.

A comprehensive comparison of the BHE thermal resistances between case *I* and case *II* requires considering also the conductive contribution in the tubes and the convective contribution of the fluid flowing inside the tubes. The conductive thermal resistance per unit length of the tube wall can be evaluated as:

$$R'_{cond} = \frac{1}{2\pi k_p} \ln \frac{D_t}{D_{ti}} \qquad (15)$$

where k_p is the thermal conductivity of the tubes and D_{ti} is the tube internal diameter. According to Ref. [6], we assume D_{ti} equal to 26.2 mm for case *I* and equal to 32.6 mm for case *II*. Thus, by considering the same material for the tubes in the two cases, the ratio between the conductive thermal resistances per unit length depends on the geometrical parameters only (we assume temperature-independent properties), namely:

$$\left(R'_{cond\ II} / R'_{cond\ I}\right) = \left(\ln \frac{D_t}{D_{ti}}\right)_{II} \Big/ \left(\ln \frac{D_t}{D_{ti}}\right)_{I} = 1.02 \qquad (16)$$

The convective thermal resistance per unit length can be evaluated as:

$$R'_{conv} = \frac{1}{h\pi D_{ti}} = \frac{D_{ti}}{Nu\, k_f \pi D_{ti}} = \frac{1}{Nu\, k_f \pi} \qquad (17)$$

where Nu is the Nusselt number and k_f is the thermal conductivity of the fluid.

By assuming that the flow regime is turbulent, one can evaluate the Nusselt number by means of the Dittus-Boelter correlation, namely:

$$Nu = 0.023\, \mathrm{Re}^{0.8}\, \mathrm{Pr}^{0.4} \qquad (18)$$

$$\text{with} \quad \mathrm{Re} = \frac{w_f D_{ti}}{\nu_f} \qquad \mathrm{Pr} = \frac{\nu_f}{\alpha_f} \qquad (19)$$

where ρ_f, ν_f, α_f are the density, the kinematic viscosity and the thermal diffusivity of the fluid, respectively. The average fluid velocity w_f in the tubes is given by:

$$w_f = \frac{4\dot{m}}{\pi \rho_f D_{ti}^2} \qquad (20)$$

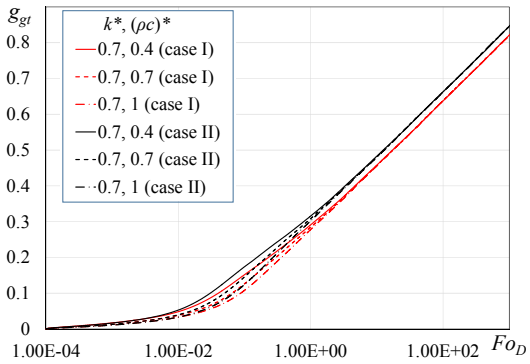

Figure 5. Comparison of the *g*-function g_{gt} between case *I* and case *II*, for $k^* = 0.7$.

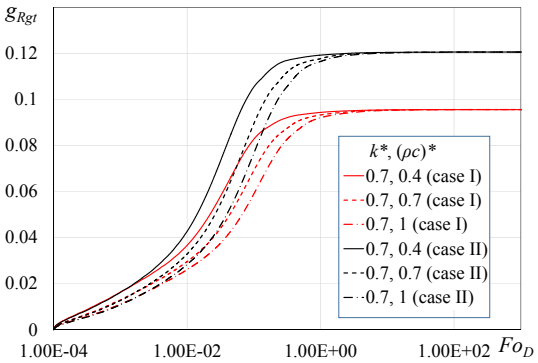

Figure 6. Comparison of the *g*-function g_{Rgt} between case *I* and case *II*, for $k^* = 0.7$.

If one assumes the same value of the mass flow rate $\dot{m}$ for both the BHE configurations (cases *I* and *II*), the ratio between the convective thermal resistances per unit length is a function of the ratio between tubes internal diameters:

$$\left(R'_{conv\ II} / R'_{conv\ I}\right) = \left(\frac{D_{ti\ II}}{D_{ti\ I}}\right)^{0.8} = 1.19 \qquad (21)$$

Since Eqs. (14), (16) and (21) show that the three contributions to the total BHE thermal resistance per unit length are bigger in case *II*, case *I* is recommendable in order to enhance the heat transfer from the BHE. However, for the sake of comparison, the previous thermal analysis should be complemented by a detailed analysis of the pressure drops in the fluid and the consequent energy consumptions for pumping.

Finally, for a single U-tube BHE let us study the effect of the distance d between the tubes on the BHE thermal response.

Figures 7 and 8 present the plots of g_{gt} and the plots of g_{Rgt}, respectively, for cases *III*, *IV* and *V*, when $k^* = 0.7$. As expected, Figure 7 shows that as the distance d increases (*i.e.*, as the tubes approach to the BHE boundary, case *V*) the dimensionless average temperature at the interface tubes-grout decreases. Indeed, accordingly to Figure 8, case *V* presents the lower dimensionless grout thermal resistance per unit length. Similar results hold for $k^* = 0.4$ and $k^* = 1$.

In order to evaluate the grout thermal resistance per unit length, R'_{gt}, of a single U-tube BHE, Paul [7] introduced the following correlation, based on experimental data:

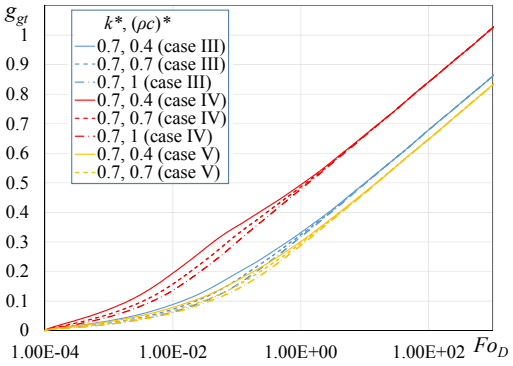

Figure 7. Comparison of the *g*-function g_{gt} in cases *III*, *IV* and *V*, for $k^* = 0.7$.

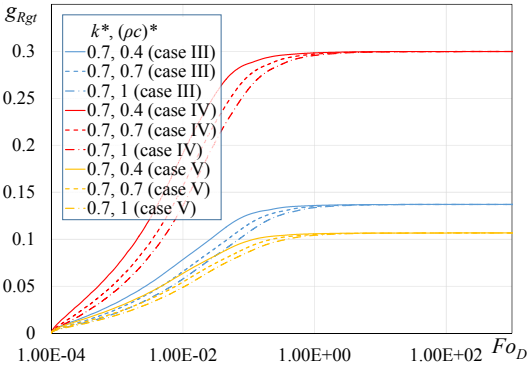

Figure 8. Comparison of the *g*-function g_{Rgt} in cases *III*, *IV* and *V*, for $k^* = 0.7$.

$$R'_{gt} = \frac{1}{\beta_0 \left(D/D_t \right)^{\beta_1} \cdot k_{gt}} \tag{22}$$

where β_0 and β_1 are constants, whose value depends on the distance d. If Eq.(22) is adopted to express the dimensionless grout thermal resistance per unit length, g_{Rgt}, one has

$$g_{Rgt} = R'_{gt} \cdot k_g = \frac{1}{k^* \cdot \beta_0 \left(1/D_t^* \right)^{\beta_1}} \tag{23}$$

Different values of β_0 and β_1, based on the shank-spacing of the tubes in the borehole are proposed in Ref.[7]: for an intermediate position, similar to case *III*, $\beta_0 = 17.44$ and $\beta_1 = -0.6052$; for tubes in direct contact, case *IV*, $\beta_0 = 20.10$ and $\beta_1 = -0.9447$; for tubes adjacent to the BHE boundary, case *V*, $\beta_0 = 21.91$ and $\beta_1 = -0.3796$. The values of g_{Rgt} obtained by means of Eq.(23) are presented in Table 3, with reference to the geometries and values of k^* investigated.

Table 3. Values of the dimensionless steady-state grout thermal resistance per unit length, g_{Rgt}, obtained by means of Paul's correlation, Eq.(23).

case *III*: intermediate shank-spacing			
k^*	0.4	0.7	1
g_{Rgt}	0.322	0.184	0.129
case *IV*: tubes in direct contact			
k^*	0.4	0.7	1
g_{Rgt}	0.439	0.251	0.176
case *V*: tubes adjacent to the BHE external boundary			
k^*	0.4	0.7	1
g_{Rgt}	0.189	0.108	0.076

To compare our results, obtained by means of 2D transient numerical simulations and presented in Table 2 (denoted now by $g_{Rgt\ num}$), with those of Table 3 (denoted now by $g_{Rgt\ Eq.(23)}$), we define the following absolute relative difference, ε_P:

$$\varepsilon_P = \left| \frac{g_{Rgt\ num} - g_{Rgt\ Eq.(23)}}{g_{Rgt\ num}} \right| \% \tag{24}$$

Although the results are not in perfect agreement, the comparison is satisfactory, being ε_P between a minimum value of 0.9% and a maximum value of 37%, with a mean value of 18.2%.

4. Conclusions

The dimensionless average temperatures at the interface tube/grout (*i.e.*, the *g*-function g_{gt}) and grout/ground (*i.e.*, the *g*-function g_b), and their difference $g_{Rgt} = g_{gt} - g_b$ (representative of the dimensionless grout thermal resistance per unit length), have been determined by means of 2D transient simulations of the BHE cross section performed through COMSOL Multiphysics 4.3b. Two double U-tube BHEs, which differ for tubes diameter, tubes spacing and borehole diameter, as well as three single U-tube BHEs, different for tubes spacing, have been considered with reference to nine couples of values of the dimensionless parameters k^* and $(\rho c)^*$.

The following main results have been obtained:

- for a given k^*, in the short-term period, as $(\rho c)^*$ increases g_{gt} decreases, while in the long-term period g_{gt} becomes independent of $(\rho c)^*$ and is a decreasing function of k^*;
- the dimensionless grout thermal resistance per unit length g_{Rgt} is a function of both k^* and $(\rho c)^*$ but reaches a constant steady-state value for specific threshold values of Fo_D;
- a comparison of the contributions to the overall BHE thermal resistance have been made for the two double U-tube BHEs considered;
- the effect of the distance between the tubes on the grout thermal resistance in a single U-tube BHE has been investigated and the results compared with a correlation available in the literature.

5. References

[1] C. Yavuzturk, J.D. Spitler, A short time step response factor model for vertical ground loop heat exchangers, *ASHRAE Transactions*, **105**, 475-485 (1999).

[2] H. Zeng, N. Diao, Z. Fang, Heat transfer analysis of boreholes in vertical ground heat exchangers, *J. Heat and Mass Transfer*, **46**, 4467-4481 (2003).

[3] D. Marcotte, P. Pasquier, On the estimation of thermal resistance in borehole thermal conductivity test, *Renewable Energy*, **33**, 2407-2415 (2008).

[4] L. Lamarche, S. Kajl, B. Beauchamp, A review of methods to evaluate borehole thermal resistances in geothermal heat-pump systems, *Geothermics*, **39**, 187-200 (2010).

[5] E. Zanchini, S. Lazzari, New *g-functions* for the hourly simulation of double U-tube borehole heat exchanger fields, *Energy*, **70**, 444–455 (2014).

[6] HakaGerodur AG, www.hakagerodur.ch

[7] N.D. Paul, The effect of grout thermal conductivity on vertical geothermal heat exchanger design and performance, Master of Science Thesis, South Dakota State University, 1996.